

Supporting Information

Long-term imaging of intranuclear Mg^{2+} dynamics in mitosis using a localized fluorescent probe

Yusuke Matsui,^{‡a} Toshiyuki Kowada,^{‡b,c} Yi Ding,^c Priya Ranjan Sahoo,^b Kazuya Kikuchi^{*a,d} and Shin Mizukami^{*b,c}

^a Graduate School of Engineering, Osaka University, Suita, Osaka 565-0871, Japan.

^b Institute of Multidisciplinary Research for Advanced Materials, Tohoku University, Sendai, Miyagi 980-8577, Japan.

^c Graduate School of Life Sciences, Tohoku University, Sendai, Miyagi 980-8577, Japan.

^d Immunology Frontier Research Center, Osaka University, Suita, Osaka 565-0871, Japan.

[‡] Y. M. and T. K. contributed equally to this work.

* Correspondence authors: Kazuya Kikuchi: kkikuchi@mls.eng.osaka-u.ac.jp, Shin Mizukami: shin.mizukami@tohoku.ac.jp

Table of contents

1. Supplementary Movie Caption

2. Supplementary Figures

3. Supporting Methods

Materials and instruments

Fluorometric analysis

Determination of dissociation constants (K_d) and detection limit

pH sensitivity

Metal-ion selectivity

Cell culture

Subcellular localization imaging of MGQ-2H(AM)

Stable cell line generation

Mg^{2+} export experiment

Responsiveness of MGQ-2H to $[Ca^{2+}]_i$

Responsiveness of MGQ-2H to Zn^{2+} influx

Mg^{2+} imaging during mitosis

Organic synthesis

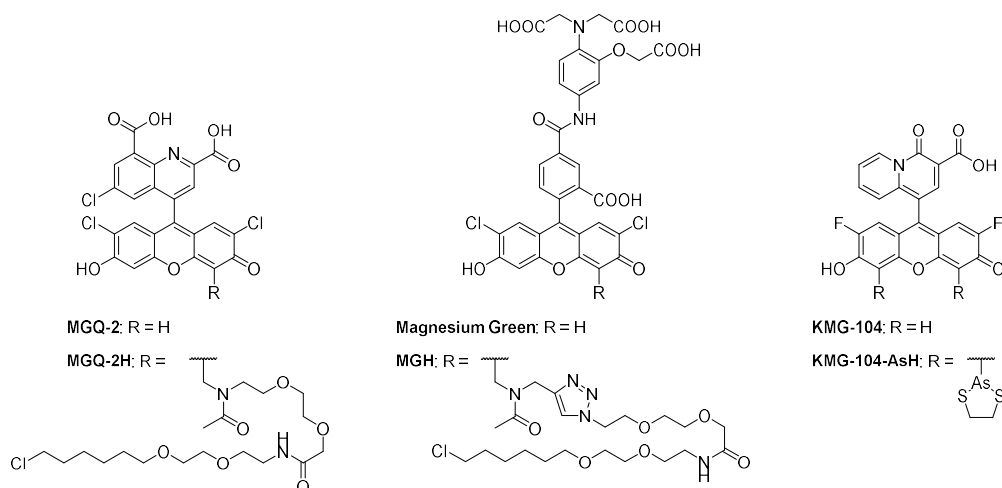
References

1. Supplementary Movie Caption

Movie S1. Confocal fluorescence imaging of intranuclear Mg^{2+} dynamics during mitosis. HEK293T cells expressing Halo-NLS were loaded with 2 μ M MGQ-2H(AM) for 30 min, followed by incubation with 1.0 μ g/mL Hoechst 33342 and 10 nM HTL-Sara650T for 15 min at 37 °C. Images were captured every 15 min in DMEM containing 10% FBS and 4.5 g/L glucose using a confocal fluorescence microscope at 37 °C and 5% CO_2 .

2. Supplementary Figures

Table S1. Spectroscopic properties of MGQ-2H and Halo-MGQ-2H^a



	λ_{abs} [nm]	λ_{em} [nm]	ϵ [cm ⁻¹ M ⁻¹]	$\Phi_{\text{free}}^{\text{b}}$ (Φ_{bound})	$K_{\text{d,Mg}}$ [mM]	$K_{\text{d,Ca}}$ [mM]	Imaging duration
MGQ-2H	524	545	81,000	0.44 (<0.01)	0.23	1.1	< 1 h
Halo-MGQ-2H	527	545	77,000	0.38 (<0.01)	0.13	0.65	24 h
MGQ-2^c	516	536	69,000	0.33 (<0.01)	0.27	1.5	< 1 h
MGH^d	515	538	77,000	0.19 (0.56)	1.3	0.012	24 h
Magnesium Green^d	509	534	77,000	0.20 (0.56)	0.88	0.012	< 2 h
KMG-104-AsH^e	521	540	44,914	<0.001 (0.001)	—	—	—
KMG-104-AsH- Tctag^{e,f}	522	541	50,680	0.006 (0.113)	1.7	>100	4 h ^g
KMG-104^e	504	523	42,000	— (0.02)	2.1	7.5	—

^a Measured at 37 °C in 100 mM HEPES buffer (pH 7.4) containing 115 mM KCl and 20 mM NaCl.

^b Relative fluorescence quantum yield determined using fluorescein ($\Phi = 0.85$ in 0.1 M NaOH aq.) as a standard. Φ_{free} and Φ_{bound} denote the relative fluorescence quantum yields in the absence and presence of Mg²⁺, respectively. ^c Data are reported in reference S1. ^d Data are reported in reference S2. ^e Data are reported in reference S3. ^f **KMG-104-AsH** conjugated with TC-tag. ^g Data is reported for the original TC-tag-FLAsH system in reference S4.

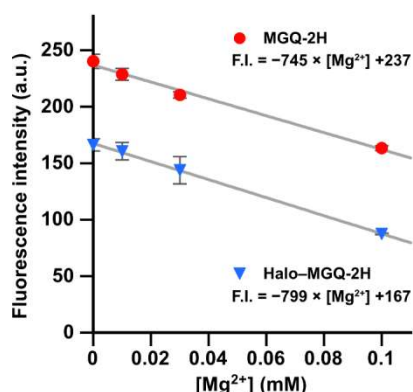


Figure S1. Changes in fluorescence intensity of MGQ-2H (red circle, $\lambda_{\text{ex}} = 524 \text{ nm}$, $\lambda_{\text{em}} = 545 \text{ nm}$) and Halo-MGQ-2H (blue triangle, $\lambda_{\text{ex}} = 527 \text{ nm}$, $\lambda_{\text{em}} = 545 \text{ nm}$) in response to Mg^{2+} . To calculate the slope of a linear fitting curve, the fluorescence intensity for Mg^{2+} concentrations between 0 to 0.1 mM from Figures 1c and S5b were plotted. The detection limits were 0.028 mM (MGQ-2H) and 0.022 mM (Halo-MGQ-2H), calculated using the following equation: Detection limit = $3.29 \times \sigma / |\text{slope}|$,^{S5} where σ is the standard deviation at 0 mM Mg^{2+} .

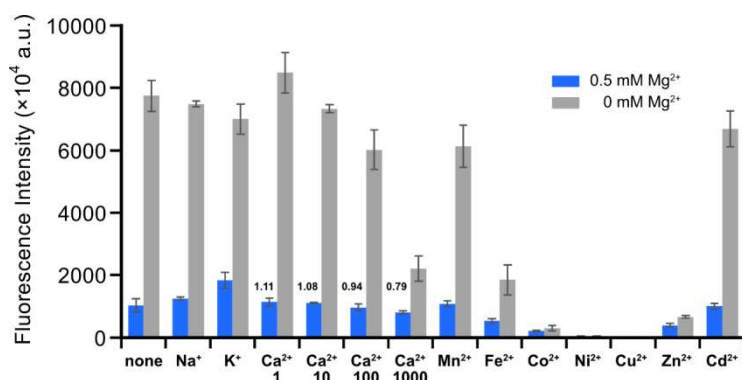


Figure S2. Metal ion selectivity of MGQ-2H. The fluorescence intensity of MGQ-2H (0.25 μM) was measured with and without Mg^{2+} (gray for 0 mM Mg^{2+} and blue for 0.5 mM Mg^{2+}) in the presence of various metal ions ($[\text{Na}^+] = 20 \text{ mM}$, $[\text{K}^+] = 115 \text{ mM}$, $[\text{Ca}^{2+}] = 1, 10, 100, \text{ or } 1000 \mu\text{M}$, $[\text{Mn}^{2+}]$, $[\text{Fe}^{2+}]$, $[\text{Co}^{2+}]$, $[\text{Ni}^{2+}]$, $[\text{Cu}^{2+}]$, $[\text{Zn}^{2+}]$, and $[\text{Cd}^{2+}] = 1 \mu\text{M}$) in 100 mM HEPES buffer (pH 7.4). Values presented above the bar graph for Ca^{2+} represent the ratio of the mean value for each Ca^{2+} concentration to the value in the absence of Ca^{2+} (none) under the 0.5 mM Mg^{2+} condition. Error bars represent SD ($n = 3$).

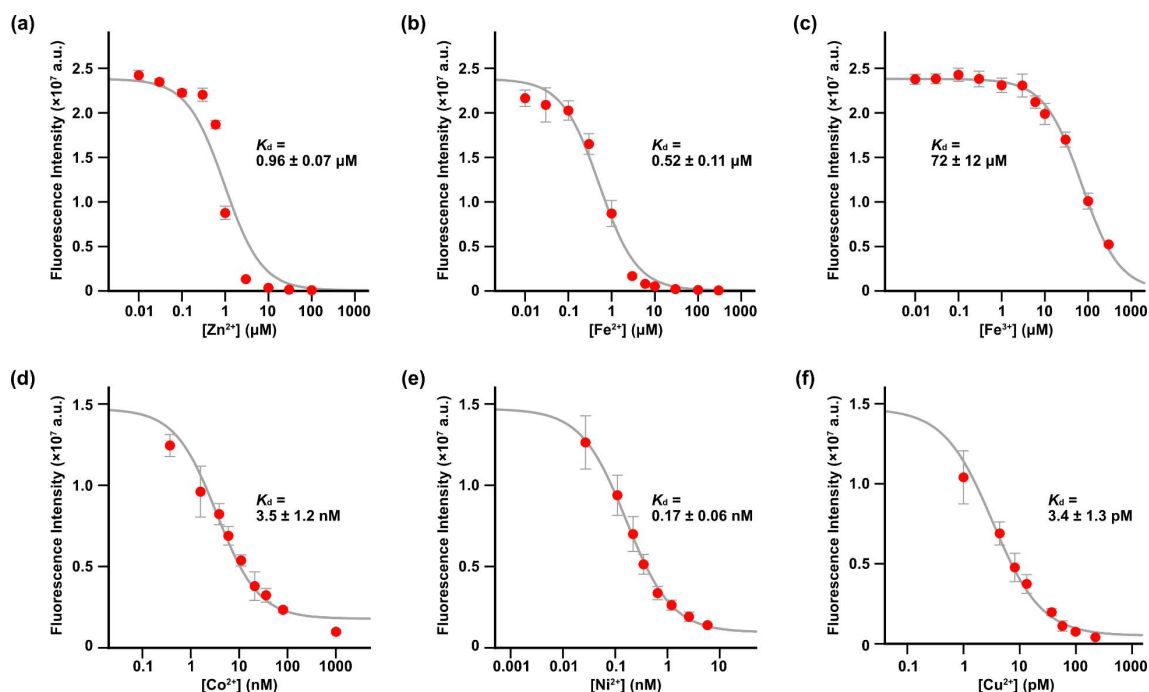


Figure S3. Fluorescence intensity changes in MGQ-2H (50 nM) as a function of $[\text{Zn}^{2+}]$ (a), $[\text{Fe}^{2+}]$ (b), $[\text{Fe}^{3+}]$ (c), $[\text{Co}^{2+}]$ (d), $[\text{Ni}^{2+}]$ (e), and $[\text{Cu}^{2+}]$ (f) in chelexed 100 mM HEPES buffer (pH 7.4, $I = 0.1$ M (NaNO_3)). (d–f) NTA-based metal ion buffers were used. Excitation at 530/30 nm. Emission at 580/20 nm. Error bars denote the standard deviation (SD) ($n = 3$).

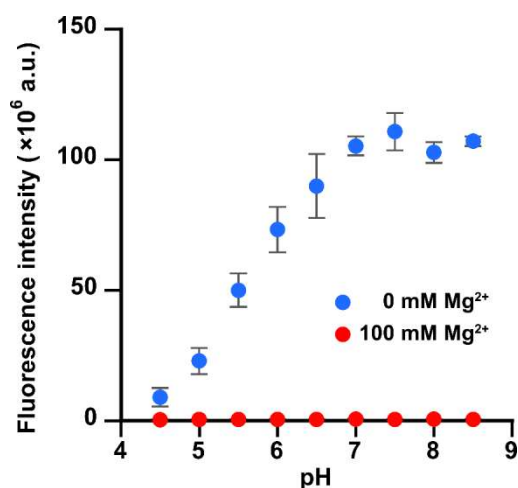


Figure S4. Effect of pH on the fluorescence intensity of MGQ-2H in a 25 mM buffer (acetate: pH 4.5–5.0, MES: pH 5.5–6.5, HEPES: pH 7.0–7.5, EPPS: pH 8.0–8.5) solution containing 115 mM KCl and 20 mM NaCl at different pH values with or without 100 mM Mg^{2+} . The measurements without Mg^{2+} were carried out in the presence of 1.0 μM EDTA to prevent the influence of a trace amount of transition metal ions. Excitation at 530/30 nm. Emission at 580/20 nm. Error bars denote the standard deviation (SD) ($n = 3$).

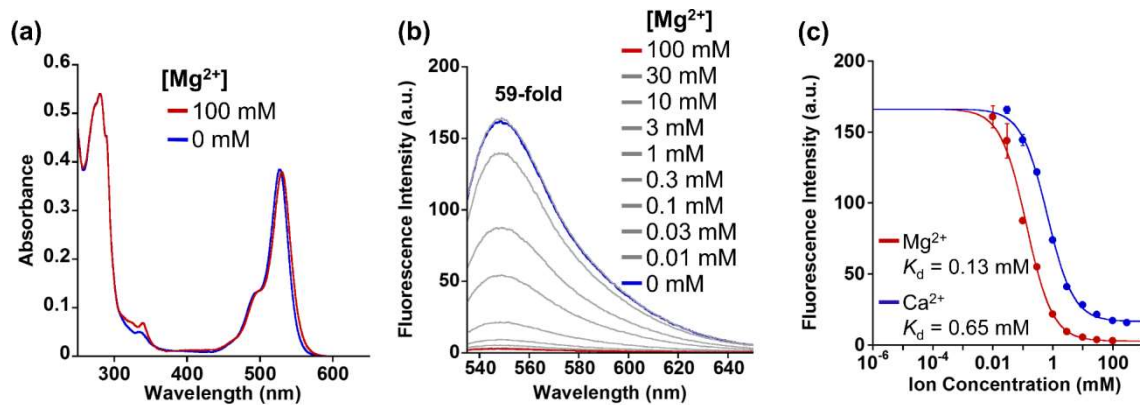


Figure S5. (a, b) Absorption (5 μM) (a) and emission (1 μM , $\lambda_{\text{ex}} = 527 \text{ nm}$) (b) spectra of HaloTag-conjugated MGQ-2H (Halo-MGQ-2H) in the presence and absence of Mg^{2+} (100 mM HEPES buffer, 115 mM KCl, 20 mM NaCl, pH 7.4, 37 $^{\circ}\text{C}$). (c) Mg^{2+} - and Ca^{2+} -titration curves of Halo-MGQ-2H fluorescence ($\lambda_{\text{ex}} = 527 \text{ nm}$, $\lambda_{\text{em}} = 545 \text{ nm}$). Error bars denote SD ($n = 3$).

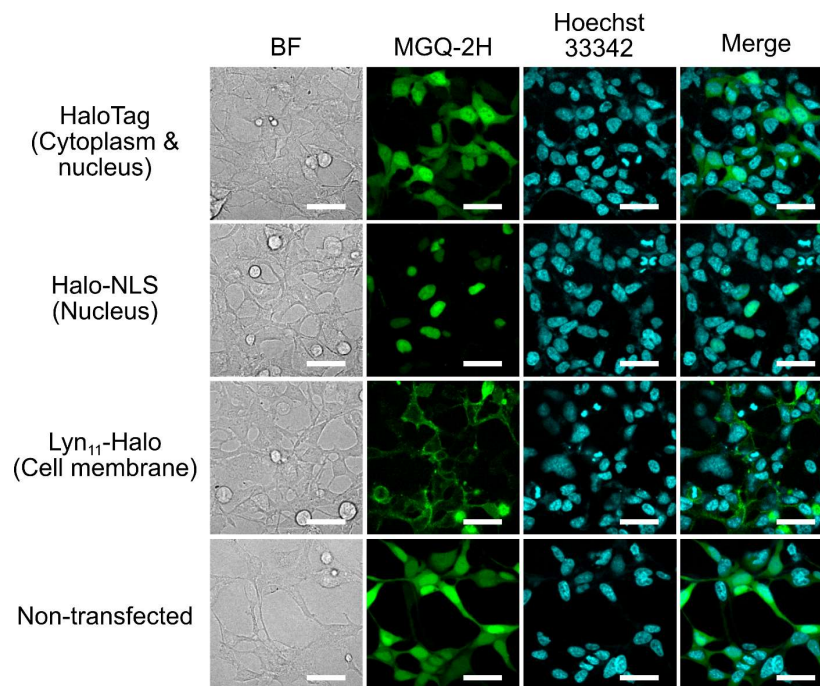


Figure S6. Confocal fluorescence microscopic images of HaloTag-expressing HEK293 cells treated with 1 μM MGQ-2H(AM) and 200 ng/mL Hoechst 33342. Scale bar: 40 μm .

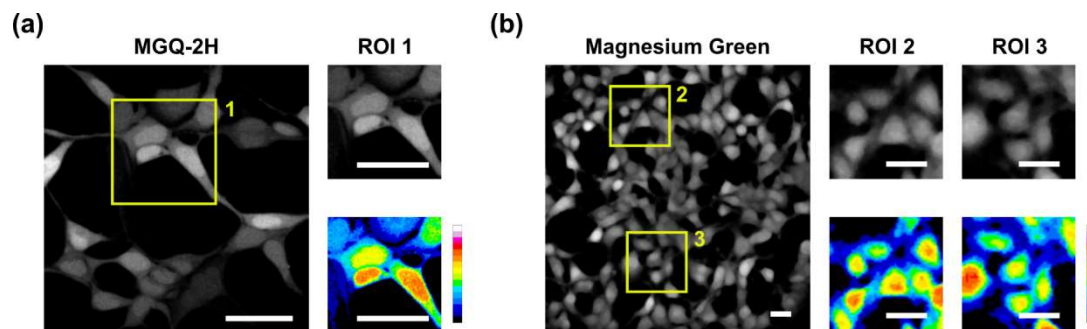


Figure S7. (a, b) Confocal fluorescence microscopic images of MGQ-2H **(a)** (same as the image of Non-transfected cells in Figure S6) and Magnesium Green **(b)** (same as the Ionomycin (-) image in Figure 2c). The magnified and pseudocolor images in the area indicated by yellow squares are presented on the right side of the original images. The contrast of images was adjusted for clarity. Scale bars: 40 μm .

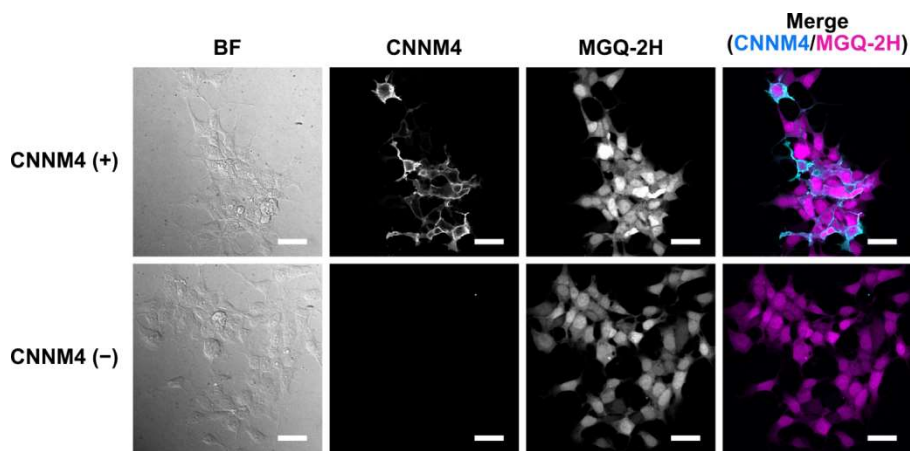


Figure S8. Confocal fluorescence microscopic images of CNNM4 (cyan) and MGQ-2H (magenta) in HEK293 cells fixed after the Mg^{2+} export experiments. Anti-FLAG antibody and CF405M conjugated goat anti-mouse antibody were used for visualizing CNNM4-FLAG, which was expressed by transient transfection of the cells. Scale bar: 40 μm .

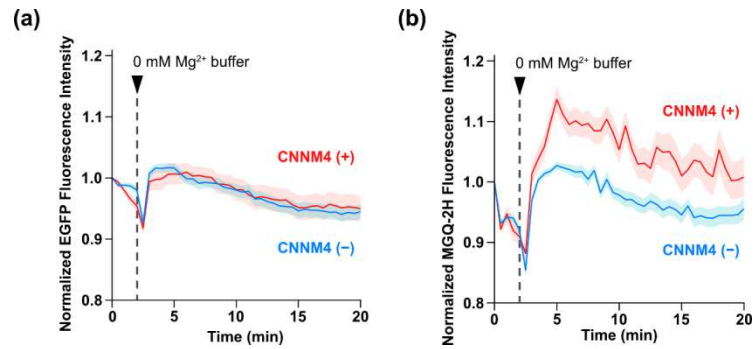


Figure S9. (a, b) Time-dependent normalized fluorescence intensity changes of Halo-EGFP **(a)** and Halo-MGQ-2H **(b)** in HEK293 cells expressing Halo-EGFP and CNNM4-FLAG. Intracellular Mg^{2+} concentration was reduced by changing extracellular Mg^{2+} concentration from 40 to 0 mM at 2 min. Solid lines and shaded area indicate mean and SEM, respectively ($n = 24$ cells, three independent experiments).

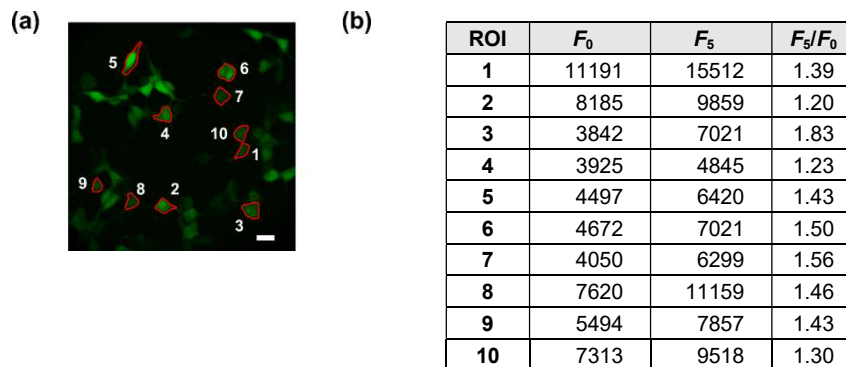


Figure S10. (a) ROIs to evaluate the changes in Halo-MGQ-2H fluorescence signal caused by the addition of ionomycin. Scale bar: 40 μ m. **(b)** The mean fluorescence signals in ROIs at 0 min (F_0) and 5 min (F_5), and the fluorescence signal ratios of these time points (F_5/F_0).

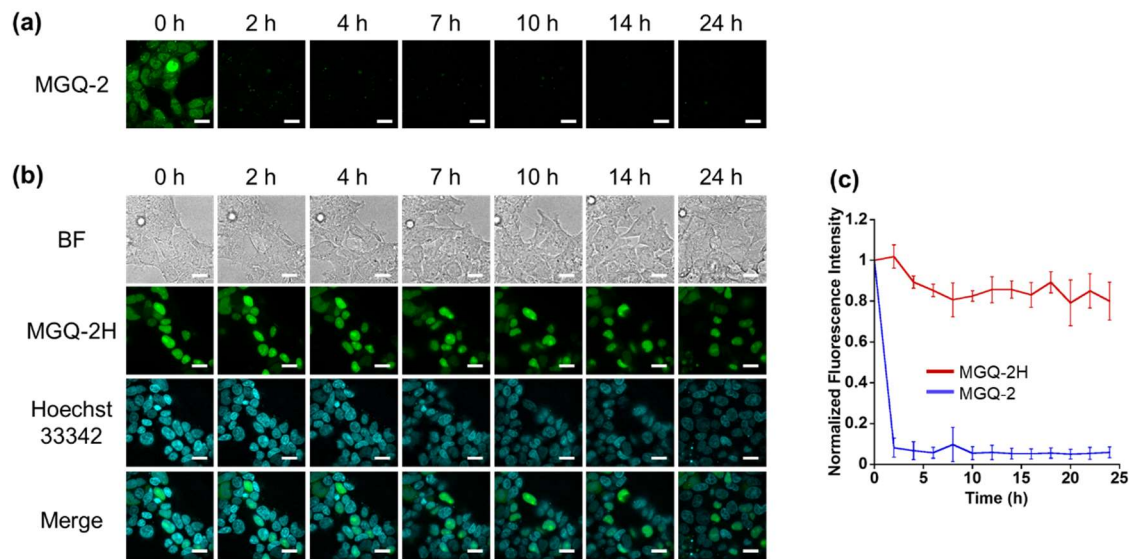


Figure S11. Comparison between **MGQ-2** and **MGQ-2H** for long-term imaging. **(a)** Long-term Mg^{2+} imaging of HEK293T cells loaded with $1 \mu M$ **MGQ-2(AM)** at $37^\circ C$ for 24 h. Scale bar: $20 \mu m$. **(b)** Long-term Mg^{2+} imaging of HEK293T cells transiently expressing Halo-NLS, loaded with $1 \mu M$ **MGQ-2H(AM)** and 200 ng/mL Hoechst 33342, at $37^\circ C$ for 24 h. Scale bar: $20 \mu m$. **(c)** Time-dependent fluorescence intensity changes of **MGQ-2H** and **MGQ-2** in a single cell. Error bars denote SD ($n = 4$).

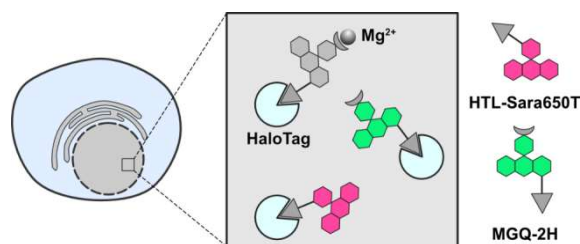


Figure S12. Illustration of ratiometric imaging principle based on simultaneous labeling of HaloTag with Mg^{2+} probe (**MGQ-2H**) and an internal standard fluorophore (**HTL-Sara650T**).

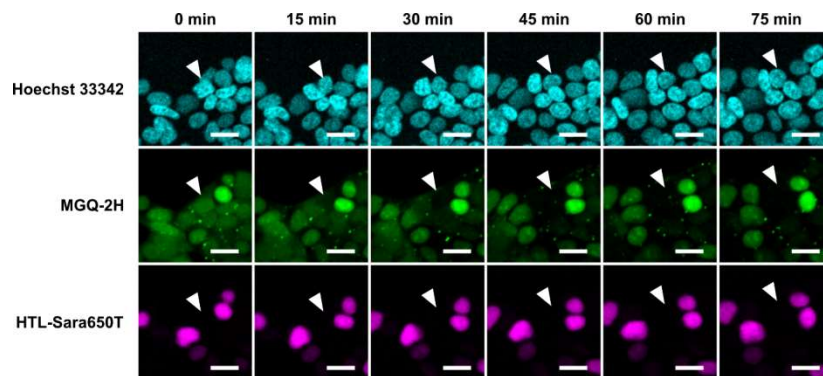


Figure S13. Confocal fluorescence microscopic images of nuclei (Hoechst), Mg^{2+} (MGQ-2H), and standard fluorophore (HTL-Sara650T) during mitosis. HEK293T cells expressing Halo-NLS were loaded with 2 μ M MGQ-2H(AM) for 30 min, followed by incubation with 1.0 μ g/mL Hoechst 33342 and 10 nM HTL-Sara650T for 15 min at 37 $^{\circ}$ C. Scale bar: 20 μ m. The MGQ-2H fluorescence signals in a cell indicated by a white arrowhead decreased to negligible levels in approximately 45 min.

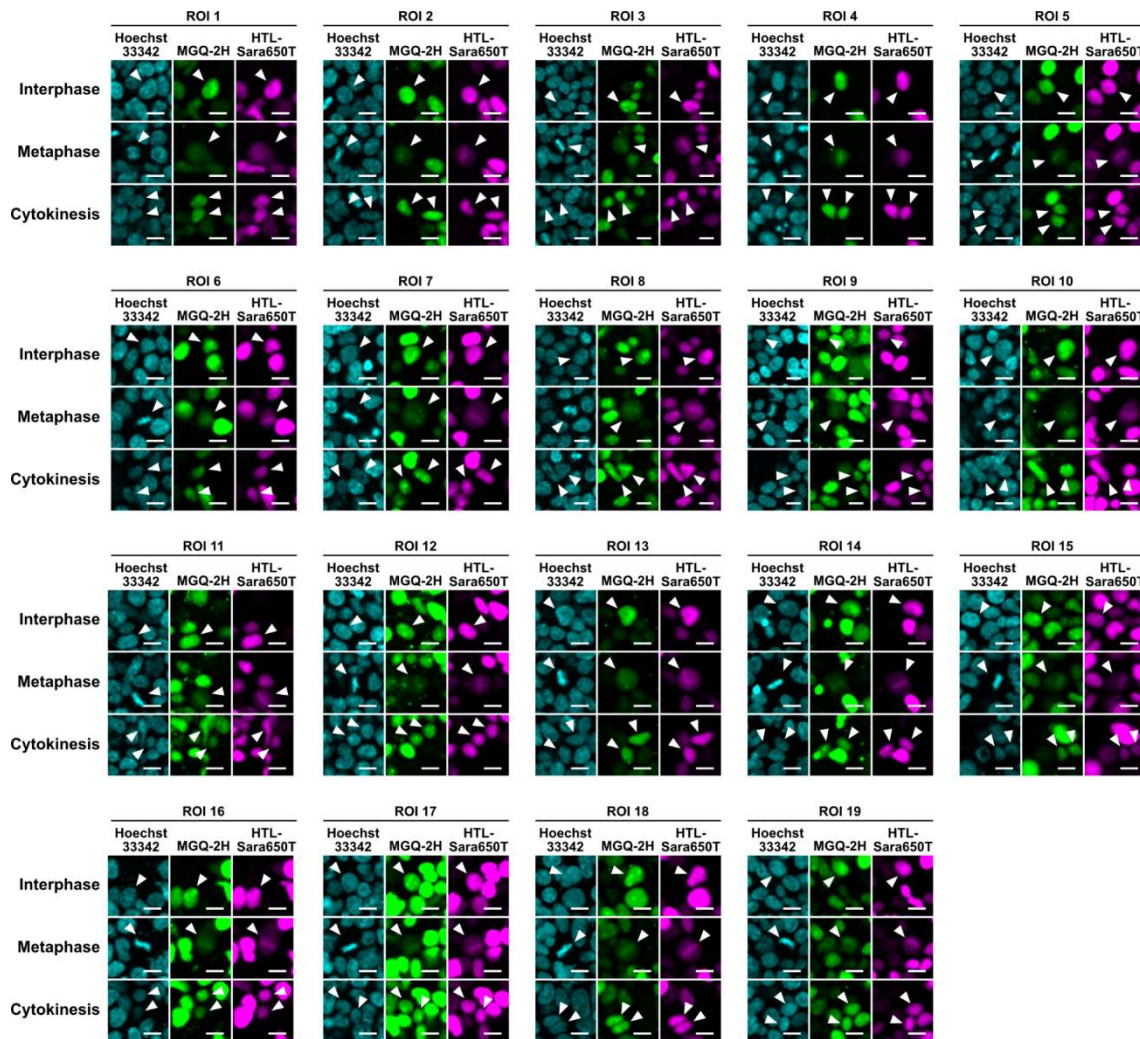


Figure S14. Confocal fluorescence microscopic images used for quantitative analysis of intranuclear Mg^{2+} dynamics during mitosis (Figure 3c). HEK293T cells expressing Halo-NLS were stained with Hoechst 33342 (cyan), MGQ-2H (green), and HTL-Sara650T (magenta). Mitotic cells were indicated by a white arrowhead. Scale bars: 15 μm .

Table S2. Normalized fluorescence ratio (F_{MGQ}/F_{Sara}) of the mitotic cells in Figure S14.

ROI	Interphase	Metaphase	Cytokinesis
1	1.00	0.638	0.819
2	1.00	0.610	1.052
3	1.00	0.715	1.069
4	1.00	0.774	1.021
5	1.00	0.785	1.014
6	1.00	0.882	0.953
7	1.00	0.759	0.988
8	1.00	0.852	1.124
9	1.00	0.822	1.036
10	1.00	0.750	1.093
11	1.00	0.811	1.048
12	1.00	0.778	0.916
13	1.00	0.850	1.049
14	1.00	0.800	1.070
15	1.00	0.839	1.077
16	1.00	0.730	0.887
17	1.00	0.714	1.040
18	1.00	0.735	0.928
19	1.00	0.800	0.990
Mean	1.00	0.77	1.01
SD	0.00	0.07	0.08

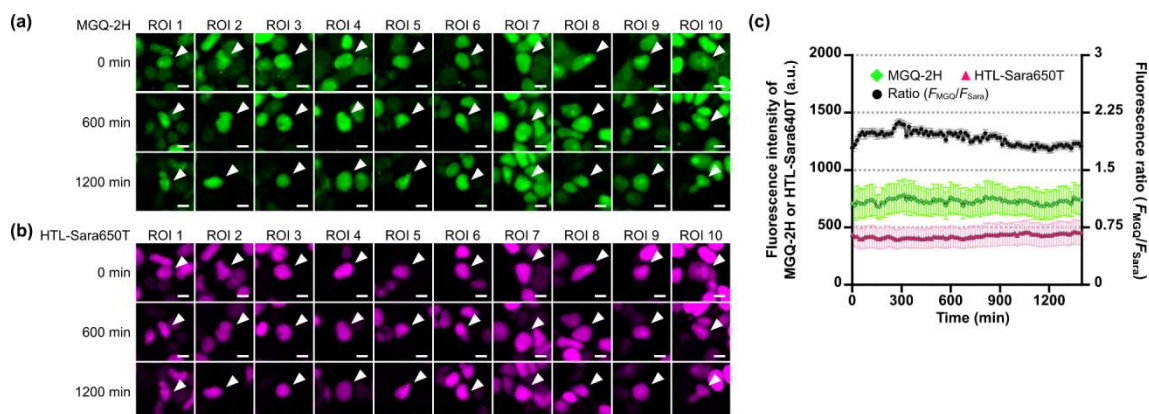


Figure S15. (a, b) Confocal fluorescence microscopic images of MGQ-2H (a) and HTL-Sara650T (b) in HEK293T cells expressing Halo-NLS. The cells were treated with 2 μM MGQ-2H(AM) for 30 min, followed by incubation with 1.0 $\mu\text{g}/\text{mL}$ Hoechst 33342 and 10 nM HTL-Sara650T for 15 min at 37 $^{\circ}\text{C}$. Scale bar: 10 μm . (c) Time course of fluorescence intensity of MGQ-2H (green, square) and HTL-Sara650T (magenta, triangle), and fluorescence ratio of MGQ-2H/HTL-Sara650T (black, circle). Error bars denote SEM ($n = 10$ cells, 3 independent experiments).

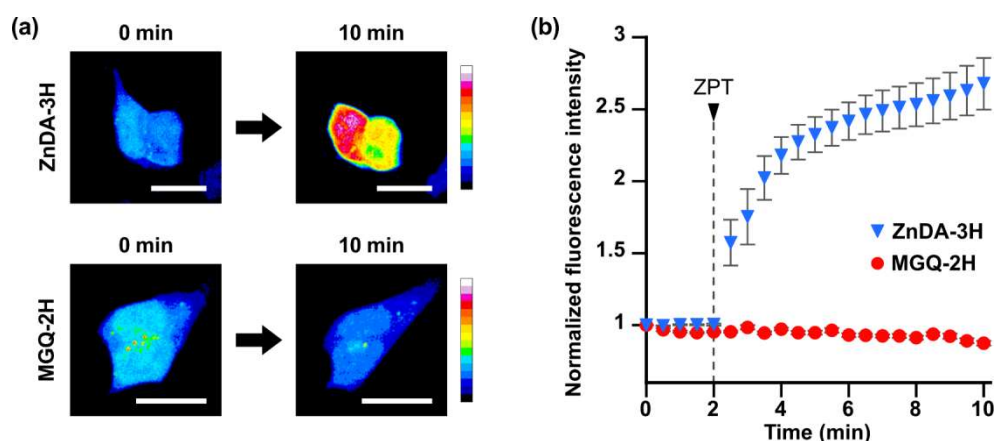


Figure S16. (a) Confocal fluorescence microscopic images of Halo-ZnDA-3H (upper) and Halo-MGQ-2H (lower) in HEK293 cells expressing HaloTag. ZnDA-3H was used to prove Zn^{2+} influx upon zinc pyrithione (ZPT: 20 μM Zn^{2+} /1.0 μM pyrithione) addition. Scale bar: 20 μm . (b) Time course of normalized fluorescence intensity of Halo-MGQ-2H (red circle) and Halo-ZnDA-3H (blue triangle) in HEK293 cells expressing HaloTag. ZPT was added at 2 min. Error bars represent SEM ($n = 16$ cells, two independent experiments).

3. Supporting Methods

Materials and instruments

General chemicals used for organic synthesis were of the best grade available, supplied by Tokyo Chemical Industries, Wako Pure Chemical Industries, or Sigma-Aldrich Chemical Co., and used without further purification. Analytical thin-layer chromatography (TLC) was performed using TLC Silica gel 60 F₂₅₄ (Merck & Co., Inc.). Silica gel column chromatography was performed using BW-300 (Fuji Silysia Chemical Ltd.). MGQ-2H and MGQ-2H(AM) were dissolved in dimethyl sulfoxide (DMSO; biochemical grade; Wako Pure Chemical Industries) before the fluorescence measurements to facilitate solubilization in an aqueous solution. Magnesium Green(AM) was purchased from Thermo Fisher Scientific. Ionomycin was purchased from Wako Pure Chemical Industries. CMV-R-GECO1.0 was purchased from Addgene (#32444). HaloTag SaraFluor 650T ligand (HTL-Sara650T, $\lambda_{\text{abs}} = 645 \text{ nm}$, $\lambda_{\text{em}} = 661 \text{ nm}$, $\epsilon = 100,000 \text{ M}^{-1}\text{cm}^{-1}$, QY = 0.39) was purchased from Goryo-Kayaku (#A308-01; same as #GCKA308 of Promega).

GPC purification was performed with a JAIGEL 1H-2H column (Japan Analytical Industry Co., Ltd.) using a GPC system comprising a pump (LC-6AD; Shimadzu) and detector (SPD-20A; Shimadzu). High-performance liquid chromatography (HPLC) analyses were performed with an Inertsil ODS-3 (4.6 mm \times 250 mm) column (GL Sciences Inc.) using an HPLC system comprising a pump (PU-2080; JASCO) and detector (MD-2010; JASCO). Preparative HPLC was performed with an Inertsil ODS-3 (10.0 mm \times 250 mm) column (GL Sciences Inc.) using an HPLC system comprising a pump (PU-2087; JASCO) and detector (UV-2075; JASCO). Buffer A contained 0.1% trifluoroacetic acid (TFA) in H₂O (for MGQ-2H(AM)) or 50 mM triethylammonium acetate (TEAA) in H₂O (for MGQ-2H); buffer B contained 0.1% TFA in acetonitrile (for MGQ-2H(AM)) or pure acetonitrile (for MGQ-2H). NMR spectra were recorded on a Bruker Avance 500 instrument at 500 MHz for ¹H NMR and 125 MHz for ¹³C NMR, using tetramethylsilane as an internal standard. Mass spectra were measured using a Waters LCT-Premier XE mass spectrometer or JMS-700 (JEOL).

Fluorescence spectra were measured using a Hitachi F7000 spectrometer. The slit widths were 2.5 nm for both excitation and emission, and the photomultiplier voltage was 700 V. UV-visible absorbance spectra were measured using a JASCO V-650 spectrophotometer.

Fluorescence microscopic images were recorded using a confocal fluorescence microscopic imaging system, including a fluorescence microscope (IX71; Olympus),

EMCCD (iXon3; Andor Technology), confocal scanning disc unit (CSU-X1; Yokogawa Electric Corporation), and a multispectral LED light source (Spectra X light engine; Lumencor). The filter sets were BP377 ± 25/DM405/BA447 ± 30 (for Hoechst 33342), BP488 ± 3/DM488/BA520 ± 17.5 (for MGQ-2H and Magnesium Green) and BP560 ± 13/DM561/BA624 ± 20 (for R-GECO1.0). For the Mg²⁺ export experiment, Zn²⁺-response imaging, and imaging of Zn²⁺ and Mg²⁺ during mitosis, a fluorescence microscope (IX83; Olympus) equipped with a CMOS camera (ORCA flash 4.0 v2 or ORCA-Fusion BT; Hamamatsu Photonics), confocal scanning disc unit (CSU-W1; Yokogawa Electric Corporation), and laser diode illuminator (LDI-7; 89 North) was used. The excitation wavelengths were 405, 470, 555, and 640 nm. The filter sets were BP402 ± 9/DM405/BA450 ± 25 (for Hoechst 33342 and CF405M), BP468 ± 7/DM488/BA525 ± 25 (for EGFP and ZnDA-3H), BP553 ± 6/DM561/BA600 ± 25 (for MGQ-2H), and BP639 ± 6/DM640/BA700 ± 37.5 (for HTL-Sara650T). The whole system was controlled using the MetaMorph 7.6 software (Molecular Devices).

Fluorometric analysis

The relative fluorescence quantum yields of the compounds were calculated using the following equation:

$$\Phi_x = \Phi_{st} (I_x/I_{st})(A_{st}/A_x)(n_x^2/n_{st}^2),$$

where Φ_{st} is the reported quantum yield of the standard, I is the integrated emission spectrum, A is the absorbance at the excitation wavelength, and n is the solvent refractive index. The subscripts, x and st, denote the sample and standard, respectively. Fluorescein ($\Phi = 0.85$ when excited at 492 nm in 100 mM NaOH aq.) was used as the standard.

Determination of dissociation constants (K_d) and detection limit

Recombinant HaloTag protein and HaloTag-conjugated MGQ-2H (Halo–MGQ-2H) were prepared by previously described procedures.^{S2} For Ca²⁺ and Mg²⁺, the fluorescence intensity ($\lambda_{em} = 545$ nm) of 1 μ M MGQ-2H ($\lambda_{ex} = 524$ nm) or 1 μ M Halo–MGQ-2H ($\lambda_{ex} = 527$ nm) was recorded at 37 °C in 100 mM HEPES buffer (pH 7.4) containing 115 mM KCl and 20 mM NaCl using a fluorometer (Hitachi F7000). For Zn²⁺, Fe²⁺, and Fe³⁺, the fluorescence intensity of 50 nM MGQ-2H was recorded at 37 °C in chelexed (Chelex, Bio-Rad Co.) 100 mM HEPES buffer (pH 7.4, $I = 0.1$ M (NaNO₃)) using microplate reader (Nivo, PerkinElmer) equipped with a 530/30 nm excitation filter, 565-nm dichroic mirror, and 580/20 nm emission filter. Metal ion-buffered solutions for Co²⁺, Ni²⁺, and Cu²⁺ containing 100 mM HEPES buffer (pH 7.4, $I = 0.1$ M (NaNO₃)) were prepared using 10 mM nitrilotriacetic acid (NTA) with different concentrations of Co²⁺, Ni²⁺, and Cu²⁺,

respectively. The composition of each metal ion-buffered solution is shown below. The free metal ion concentrations ($[M^{2+}]_{\text{free}}$) were calculated by using the following equation:^{S6}

$$[M^{2+}]_{\text{free}} = [M^{2+}]_{\text{total}} / \{\beta'_1 \times \alpha_M \times ([NTA]_{\text{total}} - [M^{2+}]_{\text{total}})\},$$

where β'_1 is the apparent stability constant for the NTA- M^{2+} complex, which is defined as $\beta'_1 = \beta_1 / (\alpha_M \times \alpha_L)$. β_1 is the stability constant for the NTA- M^{2+} complex (Co^{2+} : $10^{10.4}$; Ni^{2+} : $10^{11.5}$; Cu^{2+} : $10^{13.0}$),^{S7} $\alpha_M = 1 + 10^{(\text{pH} - \text{p}K_1)}$, and $\alpha_L = 1 + 10^{\text{p}K_{a1} - \text{pH}}$. $\text{p}K_1$ for Co^{2+} , Ni^{2+} , and Cu^{2+} are 8.9, 9.9, and 8.0, respectively, and the $\text{p}K_{a1}$ for NTA is 9.75.^{S6}

$[\text{Co}^{2+}]_{\text{total}}$ (mM)	0.40	1.5	3.0	4.0	5.5	7.0	8.0	9.0
$[\text{Co}^{2+}]_{\text{free}}$ (nM)	0.37	1.6	3.8	6.0	11	21	36	81
$[\text{Ni}^{2+}]_{\text{total}}$ (mM)	0.40	1.5	2.5	3.5	5.0	6.5	8.0	9.0
$[\text{Ni}^{2+}]_{\text{free}}$ (nM)	0.027	0.11	0.22	0.35	0.65	1.2	2.6	5.8
$[\text{Cu}^{2+}]_{\text{total}}$ (mM)	0.40	1.5	2.5	3.5	6.0	7.0	8.0	9.0
$[\text{Cu}^{2+}]_{\text{free}}$ (pM)	1.0	4.4	8.2	13	37	58	99	222

Fluorescence intensity at 1 μM Co^{2+} was measured in chelexed 100 mM HEPES buffer (pH 7.4, $I = 0.1$ M (NaNO_3)) by adding 1 μM Co^{2+} in the absence of NTA, as this is outside the buffering range of NTA. The fluorescence intensity was plotted against various concentrations of target metal ions ($[\text{Mg}^{2+}]$: 0.01–100 mM, $[\text{Ca}^{2+}]$: 0.01–300 mM, $[\text{Ca}^{2+}]$: 0.01–300 mM, $[\text{Zn}^{2+}]$: 0.01–100 μM , $[\text{Fe}^{2+}]$: 0.01–300 μM , $[\text{Fe}^{3+}]$: 0.01–300 μM , $[\text{Co}^{2+}]$: 0.37 nM–1.0 μM , $[\text{Ni}^{2+}]$: 0.027–5.8 nM, $[\text{Cu}^{2+}]$: 1.0–222 pM), and the K_d was calculated using the following equation:

$$[M] = K_d (F - F_{\text{free}}) / (F_{\text{sat}} - F),$$

where $[M]$ is the concentration of the free target metal ion, F , F_{free} , and F_{sat} are the fluorescence intensities at each metal ion concentration, before adding the metal ion, and at the saturation point, respectively. The F_{sat} values (2.38×10^7 for Zn^{2+} , Fe^{2+} , and Fe^{3+} ; 1.47×10^7 for Co^{2+} , Ni^{2+} , and Cu^{2+}) were determined by measuring the fluorescence intensity in the absence of metal ions.

To determine the detection limits of MGQ-2H and Halo-MGQ-2H for Mg^{2+} concentrations, the fluorescence intensities measured at Mg^{2+} concentrations of 0, 0.01, 0.03, and 0.1 mM were plotted. The slope value of the linear fitting curve to the plot was used to calculate the detection limits using the following equation:^{S5}

$$\text{Detection limit} = 3.29 \times \sigma / |\text{slope}|,$$

where σ is the standard deviation at 0 mM Mg^{2+} .

pH sensitivity

Twenty-five μM of MGQ-2H in DMSO was diluted to 0.25 μM in 25 mM pH buffer containing 115 mM KCl and 20 mM NaCl at different pH values using appropriate buffer (acetate: pH 4.5 and 5.0; MES: pH = 5.5, 6.0, and 6.5; HEPES: pH 7.0 and 7.5; EPPS: pH 8.0 and 8.5) with or without 100 mM MgCl_2 . The measurements without Mg^{2+} were carried out in the presence of 1.0 μM EDTA to prevent the influence of a trace amount of transition metal ions. The fluorescence intensity was recorded at 37 °C using a microplate reader (Nivo, PerkinElmer) equipped with a 530/30 nm excitation filter, a 565-nm dichroic mirror, and a 580/20 nm emission filter.

Metal-ion selectivity

Twenty-five μM of MGQ-2H in DMSO was diluted to 0.25 μM in 100 mM HEPES buffer (pH 7.4) in the presence of various metal ions ($[\text{NaCl}] = 20$ mM, $[\text{KCl}] = 115$ mM, $[\text{CaCl}_2] = 1, 10, 100, \text{ or } 1000$ μM , $[\text{MnCl}_2]$, $[\text{FeCl}_2]$, $[\text{CoCl}_2]$, $[\text{NiCl}_2]$, $[\text{CuCl}_2]$, $[\text{ZnSO}_4]$, and $[\text{CdCl}_2] = 1$ μM) with or without 0.5 mM MgCl_2 . The fluorescence intensity was recorded at 37 °C using a microplate reader (Nivo, PerkinElmer) equipped with a 530/30 nm excitation filter, a 565-nm dichroic mirror, and a 580/20 nm emission filter.

Cell culture

HEK293 and HEK293T cells were cultured in high-glucose Dulbecco's modified Eagle's medium (DMEM) plus Gluta Max-I supplemented with 10% fetal bovine serum (FBS), 100 U/mL penicillin, and 100 $\mu\text{g}/\text{mL}$ streptomycin. Cells were incubated at 37 °C in a humidified atmosphere containing 5% CO_2 . Subculture was performed every 2–3 d from subconfluent (<80%) cultures using a trypsin–ethylenediaminetetraacetic acid solution. Transfection of plasmids was carried out in a glass-bottomed dish using Lipofectamine 3000 or FuGENE HD according to the standard protocol.

Subcellular localization imaging of MGQ-2H(AM)

HEK293 or HEK293T cells maintained in 10% FBS in DMEM at 37 °C and 5% CO_2 were transfected with pcDNA3.1(+)-Halo-NLS, pcDNA3.1(+)-Lyn₁₁-Halo, or pcDNA3.1(+)-HaloTag plasmids using Lipofectamine 3000, and the cells were incubated at 37 °C for 24 h. Then, the cells were washed three times with Hanks' balanced salt solution (HBSS) and incubated in FBS-free DMEM containing 1 μM MGQ-2H(AM) for 45 min in a CO_2 incubator. After washing with HBSS, the fluorescence images were captured in FBS-free DMEM using a confocal fluorescence microscope at 37 °C.

Stable cell line generation

To construct pcDNA3.1-Halo-EGFP, the gene encoding EGFP was cloned into the pcDNA3.1-Halo-mCherry vector at the HindIII/EcoRI (mCherry) site.^{S8} HEK293 cells stably expressing Halo-EGFP were created by transfection of a linearized DNA, which was prepared by treating pcDNA3.1-Halo-EGFP with ScaI. For neomycin-resistance, selection was carried out with G418 (#09380-86, Nacalai Tesque) for 3 weeks, after which colonies were picked up.

Mg²⁺ export experiment

For the condition of CNNM4 (+), HEK293 cells stably expressing Halo-EGFP were transfected with pCMV-CNNM4-FLAG using FuGENE HD, and the cells were incubated at 37 °C for 24 h. Cells were then incubated with Mg²⁺-loading buffer (78.1 mM NaCl, 5.4 mM KCl, 1.8 mM CaCl₂, 40 mM MgCl₂, 5.5 mM glucose, 5.5 mM HEPES-KOH, pH 7.4), including 2 μM MGQ-2H(AM) for 45 min at 37 °C. The cells were rinsed once with Mg²⁺-loading buffer, and fluorescence images were captured every 30 s for 20 min using a confocal fluorescence microscope. The buffer was then changed to Mg²⁺-free buffer (MgCl₂ in the loading buffer was replaced with 60 mM NaCl). For the condition of CNNM4 (-), the same experiments were performed without the transient transfection.

To quantitatively analyze the response of Halo-MGQ-2H to Mg²⁺ depletion from the extracellular solution, eight cells were picked up from each of the three independent experiments. In particular, for the condition of CNNM4 (+), the cells with a significant fluorescence signal change were picked up.

After the time-lapse imaging, the imaging buffer was removed. The cells were fixed with 4% paraformaldehyde in PBS for 15 min, permeabilized with 0.1 % Triton X-100 in PBS for 15 min, and blocked with 3% BSA in PBS for 50 min. After staining with anti-FLAG mouse monoclonal antibody (1:1000, #018-22381, FUJIFILM Wako Pure Chemical Corporation) and CF405M goat anti-mouse IgG (1:1000, #20180-1, Biotium), the confocal fluorescence images were obtained.

Responsiveness of MGQ-2H to [Ca²⁺]_i

HEK293 cells were transfected with pcDNA3.1-Halo or pCMV-R-GECO1.0 using Lipofectamine 3000, and the cells were incubated at 37 °C for 24 h. Then, the cells were incubated in FBS-free DMEM containing 1 μM MGQ-2H(AM) or 1 μM Magnesium Green(AM) for 45 min at 37 °C. The cells were rinsed twice with Mg²⁺- and Ca²⁺-free HEPES-buffered Hanks' balanced salt solution (HHBSS), and 10 mM Ca²⁺ in Mg²⁺-free HHBSS was added to the cells. Time-lapse images were obtained after the addition of 5

μM ionomycin after 1 min. Fluorescence images were captured every 20 s using a confocal fluorescence microscope.

Responsiveness of MGQ-2H to Zn^{2+} influx

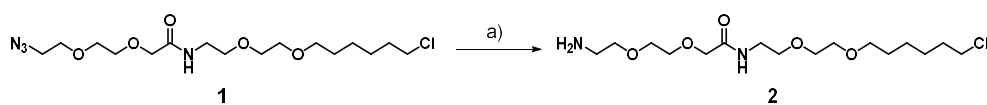
HEK293 cells were transfected with pcDNA3.1-Halo using FuGENE HD, and the cells were incubated at 37 °C for 24 h. The cells were then incubated in FBS-free DMEM containing 2 μM MGQ-2H(AM) or 0.25 μM ZnDA-3H for 45 min at 37 °C. After washing the cells once with HBSS (+), time-lapse imaging was performed in 1.8 mL HBSS (+) using a confocal fluorescence microscope with 30 s intervals for 10 min. At 2 min, 200 μL of HBSS (+) containing 200 μM ZnSO_4 and 10 μM pyrithione (final concentrations of 20 μM Zn^{2+} and 1 μM pyrithione) was added.

Mg^{2+} imaging during mitosis

HEK293T cells maintained in 10% FBS in DMEM at 37 °C and 5% CO_2 were transfected with pcDNA3.1(+)-Halo-NLS plasmid using FuGENE HD. After 24 h, the cells were washed twice with HBSS (+), incubated with 2 μM MGQ-2H(AM) for 30 min, and treated with 1 $\mu\text{g}/\text{mL}$ Hoechst 33342 and 10 nM HaloTag SaraFluor 650T ligand (HTL-Sara650T) for 15 min at 37 °C and 5% CO_2 . After washing twice with HBSS (+), fluorescence images were captured every 15 min in DMEM containing 10% FBS and 4.5 g/L glucose using a confocal fluorescence microscope at 37 °C and 5% CO_2 .

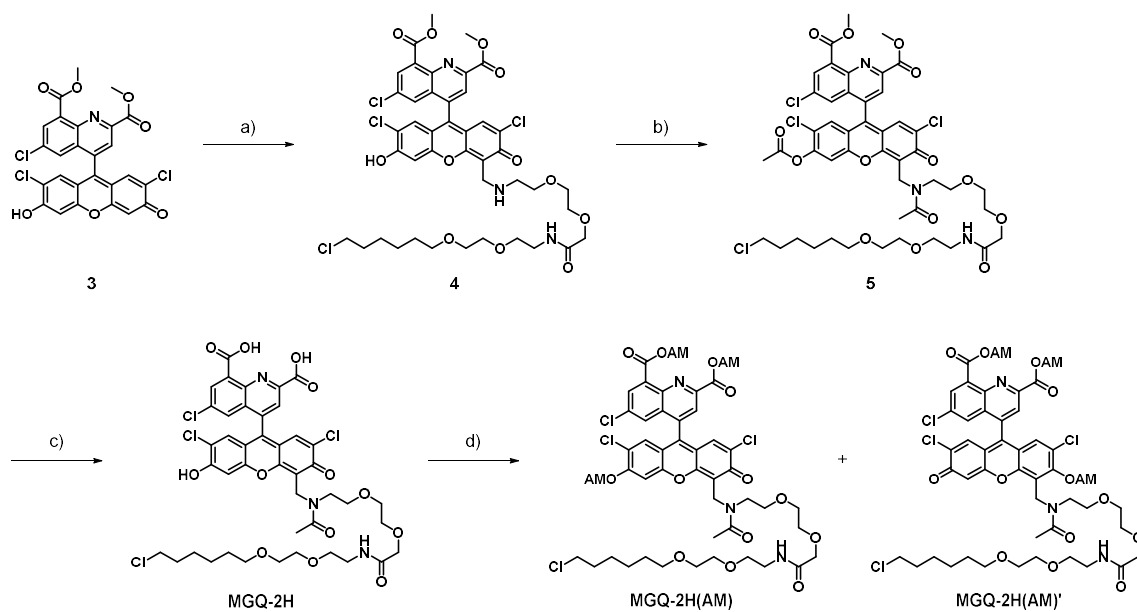
For the stochastic analysis, two-tailed paired Student's *t*-tests were performed.

Organic synthesis



Scheme S1. Synthesis of a HaloTag ligand.

a) Pd/C, H_2 , MeOH, r.t., quant.



Scheme S2. Synthesis of MGQ-2H and its cell-permeable derivatives.

a) compound **2**, paraformaldehyde, CH₃CN/H₂O (1:1), 90 °C; b) pyridine, Ac₂O, DMF, r.t.; c) 2 M NaOH aq., MeOH/H₂O (3:1), r.t., 18% (3 steps); d) bromomethyl acetate, DIEA, DMF, r.t., 16% obtained as a 1:1 mixture of the diastereomers.

Synthesis of compound 2

Compound **1**^{S1} (25.0 mg, 63.3 μmol) was dissolved in MeOH (2 mL). Pd/C (20%, 5.00 mg) was added, and the reaction mixture was stirred for 2 h under H₂. The reaction mixture was filtered through a layer of celite and evaporated under reduced pressure. Compound **2** (23.4 mg, 63.4 μmol, quant.) was obtained as a colorless oil.

¹H NMR (500 MHz, CDCl₃) δ 7.18 (br s, 1H), 4.02 (s, 2H), 3.70–3.45 (m, 18H), 2.92 (t, *J* = 5.0 Hz, 2H), 2.10 (br s, 2H), 1.81–1.75 (m, 2H), 1.63–1.57 (m, 2H), 1.49–1.43 (m, 2H), 1.40–1.35 (m, 2H); ¹³C NMR (125 MHz, CDCl₃) δ 170.0, 72.9, 71.3, 71.0, 70.6, 70.3, 70.1, 70.0, 69.9, 45.1, 41.6, 38.7, 32.5, 29.5, 26.7, 25.4; HRMS (FAB⁺): Calcd for C₁₆H₃₄³⁵ClN₂O₅⁺ [M+H]⁺ 369.2151, found 369.2158.

Synthesis of compound 4

Compound **2** (23.4 mg, 63.0 μmol) was mixed with paraformaldehyde (12.6 mg, 0.420 mmol) in 2 mL of acetonitrile under N₂ and heated to reflux for 1 h. The suspension of compound **3**^{S2} (29.3 mg, 52.5 μmol) in 2 mL of MeCN and 2 mL of H₂O was added to the reaction mixture. The mixture was refluxed for 48 h. After cooling, the solvent was removed under reduced pressure, and the residue was purified using flash column

chromatography on silica gel (DCM/MeOH, from 99:1 to 85:15). Compound **4** (14.8 mg) was obtained as an orange solid was used in the following synthesis without further purification.

MS (ESI⁺): Calcd for C₄₃H₄₈³⁵Cl₄N₃O₁₂⁺ [M+H]⁺ 938.20, found 938.14.

Synthesis of compound **5**

Compound **4** (14.8 mg) and pyridine (5.10 μL, 5.00 mg, 63.2 μmol) were stirred in dry DMF (4 mL) at room temperature for 30 min. Acetic anhydride (6.00 μL, 6.48 mg, 63.5 μmol) was added to the reaction solution. After stirring for 4 h, the solvent was removed under reduced pressure. The residue was dissolved in ethyl acetate and washed with 10% citric acid. The organic layer was dried over Na₂SO₄ and evaporated under reduced pressure. The crude mixture of compound **5** was used in the next step without further purification.

Synthesis of MGQ-2H

The crude mixture of compound **5** was dissolved in MeOH/H₂O (3:1) (4 mL), and 2 M NaOH aq. (1 mL) was added dropwise at 0 °C. The reaction mixture was warmed to room temperature and stirred for 15 h. The solution was acidified with 2 M HCl aq. and was extracted with ethyl acetate. The combined organic extracts were dried over Na₂SO₄ and evaporated under reduced pressure. The residue was purified using reversed-phase HPLC under the following conditions: A/B = 25/75 (0 min), 45/55 (30 min) (solvent A: MeCN; solvent B: 50 mM TEAA). After lyophilization, MGQ-2H·Et₃N (10.0 mg, 9.48 μmol, 18% (3 steps)) was obtained as a purple powder.

¹H NMR (500 MHz, DMSO-*d*₆) δ 8.48 (s, 1H), 8.23 (s, 1H), 8.01 (s, 1H), 7.69–7.65 (m, 1H), 6.79 (s, 2H), 6.37 (s, 1H), 4.88–4.64 (m, 2H), 3.88 (s, 2H), 3.60–3.12 (m, 20H), 3.10 (q, *J* = 7.0 Hz, 6H), 2.40 (s, 3H), 1.68–1.65 (m, 2H), 1.46–1.43 (m, 2H), 1.34–1.33 (m, 2H), 1.28–1.26 (m, 2H), 1.19 (t, *J* = 7.0 Hz, 9H); ¹³C NMR (125 MHz, DMSO-*d*₆) δ 173.5, 170.4, 169.64, 169.59, 165.9, 164.8, 156.6, 154.9, 144.1, 143.3, 143.1, 134.7, 133.8, 129.0, 128.8, 128.2, 127.1, 126.8, 126.6, 124.2, 111.3, 111.2, 109.4, 109.1, 104.2, 104.1, 70.7, 70.6, 70.5, 70.4, 70.2, 70.0, 69.9, 69.8, 69.3, 68.0, 46.0, 45.8, 38.43, 32.5, 29.5, 26.6, 25.4, 22.6, 9.1; HRMS (FAB⁺): Calcd for C₄₃H₄₆³⁵Cl₄N₃O₁₃⁺ [M+H]⁺ 952.1779, found 952.1790.

Synthesis of MGQ-2H(AM)

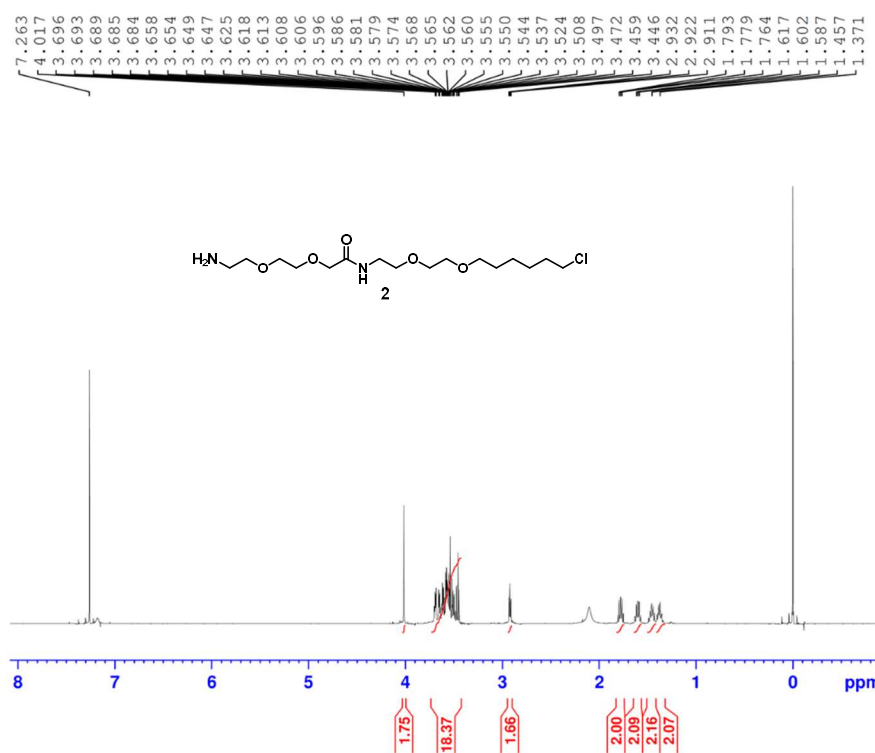
To a flame-dried three-necked flask placed under N₂, MGQ-2H·Et₃N (8.53 mg, 8.09 μmol) and DMF (1.5 mL) were added. DIEA (12.3 μL, 9.25 mg, 71.6 μmol) and

bromomethyl acetate (7.00 μ L, 11.4 mg, 74.6 μ mol) were added at room temperature. After stirring for 24 h, the solvent was removed under reduced pressure, and ethyl acetate was added to the residue. The organic layer was washed with water and brine, dried over Na_2SO_4 , and evaporated. The residue was purified using reversed-phase HPLC under the following conditions: A/B = 60/40 (0 min), 70/30 (30 min) (solvent A: 0.1% TFA in MeCN; solvent B: 0.1% TFA in H_2O). MGQ-2H(AM) (1.56 mg, 1.33 μ mol, 16%) was obtained as an orange solid (1:1 mixture of MGQ-2H(AM) and MGQ-2H(AM)').

^1H NMR (500 MHz, CD_3CN) δ 8.23 (d, 1H), 8.14 (t, $J = 2.0$ Hz, 1H), 7.86 (dd, $J = 13.0$, 2.3 Hz, 1H), 7.53 (d, $J = 13.0$ Hz, 1H), 7.21 (br s, 1H), 7.15 (d, $J = 12.4$ Hz, 1H), 7.05 (d, $J = 5.9$ Hz, 1H), 6.08 (s, 2H), 6.05 (s, 2H), 5.98 (s, 2H), 4.95–4.85 (m, 2H), 3.93 (s, 2H), 3.74–3.36 (m, 20H), 2.21–2.20 (m, 6H), 2.16 (s, 3H) 2.13 (s, 3H), 1.77–1.71 (m, 2H), 1.54–1.49 (m, 2H), 1.44–1.38 (m, 2H), 1.36–1.29 (m, 2H); ^{13}C NMR (125 MHz, CD_3CN) δ 177.3, 170.3, 170.2, 170.14, 170.12, 165.2, 163.5, 157.5, 156.2, 153.3, 148.6, 144.2, 143.2, 140.61, 140.57, 135.72, 135.69, 135.1, 132.7, 129.4, 129.2, 129.1, 128.0, 127.7, 124.4, 121.4, 120.7, 116.3, 104.1, 104.0, 85.9, 85.7, 81.1, 80.6, 71.3, 71.2, 70.8, 70.5, 70.4, 70.3, 69.81, 69.75, 45.8, 42.7, 38.9, 32.9, 29.8, 26.9, 25.7, 20.7, 20.6, 20.5; HRMS (FAB $^+$): Calcd for $\text{C}_{52}\text{H}_{57}^{35}\text{Cl}_4\text{N}_3\text{NaO}_{19}^+$ [M+Na] $^+$ 1190.2233, found 1190.2249.

References

- S1) Y. Matsui, K. K. Sadhu, S. Mizukami and K. Kikuchi, *Chem. Commun.*, 2017, **53**, 10644–10647.
- S2) Y. Matsui, Y. Funato, H. Imamura, H. Miki, S. Mizukami and K. Kikuchi, *Chem. Sci.*, 2017, **8**, 8255–8264.
- S3) Y. Hiruta, Y. Shindo, K. Oka and D. Citterio, *Chem. Lett.*, 2021, **50**, 870–887.
- S4) B. A. Griffin, S. R. Adams and R. Y. Tsien, *Science*, 1998, **281**, 269–272.
- S5) L. A. Currie, *Pure. Appl. Chem.*, 1995, **67**, 1699–1723.
- S6) D. D. Perrin and B. Dempsey, (1974), *Buffers for pH and Metal Ion Control* (John Wiley & Sons, Chapman and Hall).
- S7) G. Anderegg, *Pure. Appl. Chem.*, 1982, **54**, 2693–2758.
- S8) T. Kowada, K. Arai, A. Yoshimura, T. Matsui, K. Kikuchi and S. Mizukami, *Angew. Chem. Int. Ed.*, 2021, **60**, 11378–11383.



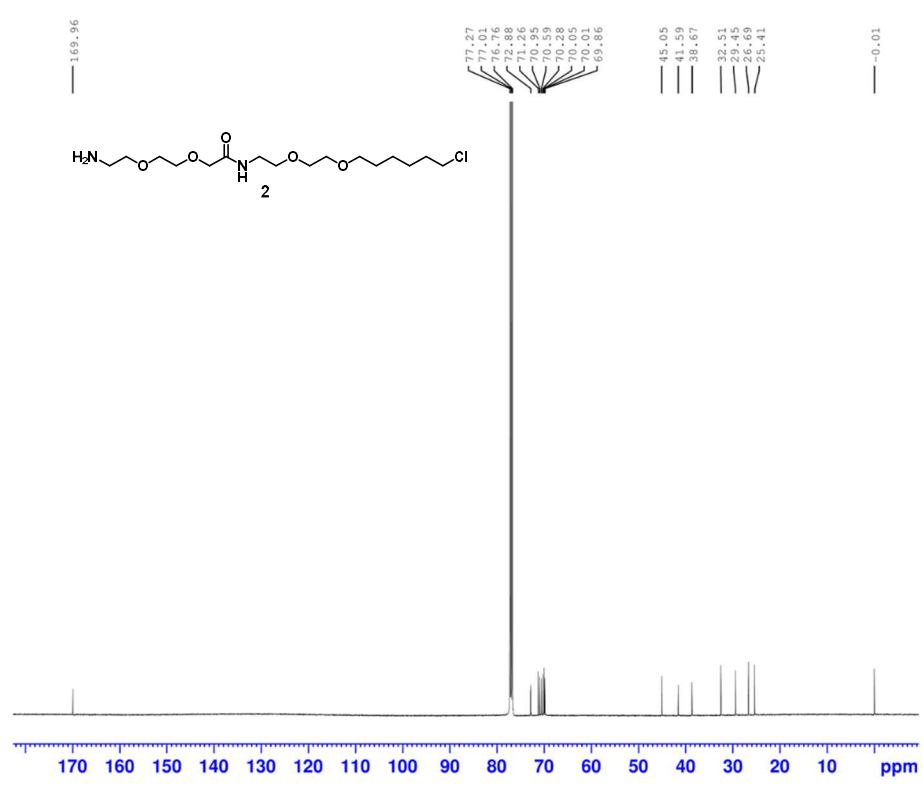
Current Data Parameters
 NAME 20180118compound122
 EXPNO 1
 PROCNO 1

F2 - Acquisition Parameters
 Date_ 20180118
 Time 21.18
 INSTRUM spect
 PROBHD 5 mm CPPBBO BB
 PULPROG zg30
 TD 65536
 SOLVENT CDC13
 NS 16
 DS 2
 SWH 10000.000 Hz
 FIDRES 0.152588 Hz
 AQ 3.2767999 sec
 RG 62.19
 DW 50.000 usec
 DE 10.00 usec
 TE 298.2 K
 D1 1.00000000 sec
 TD0 1

----- CHANNEL f1 -----
 SFO1 500.1530886 MHz
 NUC1 1H
 P1 15.00 usec
 PLW1 12.30000019 W

F2 - Processing parameters
 SI 65536
 SF 500.1500100 MHz
 WDW EM
 SSB 0
 LB 0.30 Hz
 GB 0
 PC 1.00

¹H NMR spectrum of compound 2



Current Data Parameters
 NAME 20180118compound122 13C
 EXPNO 10
 PROCNO 1

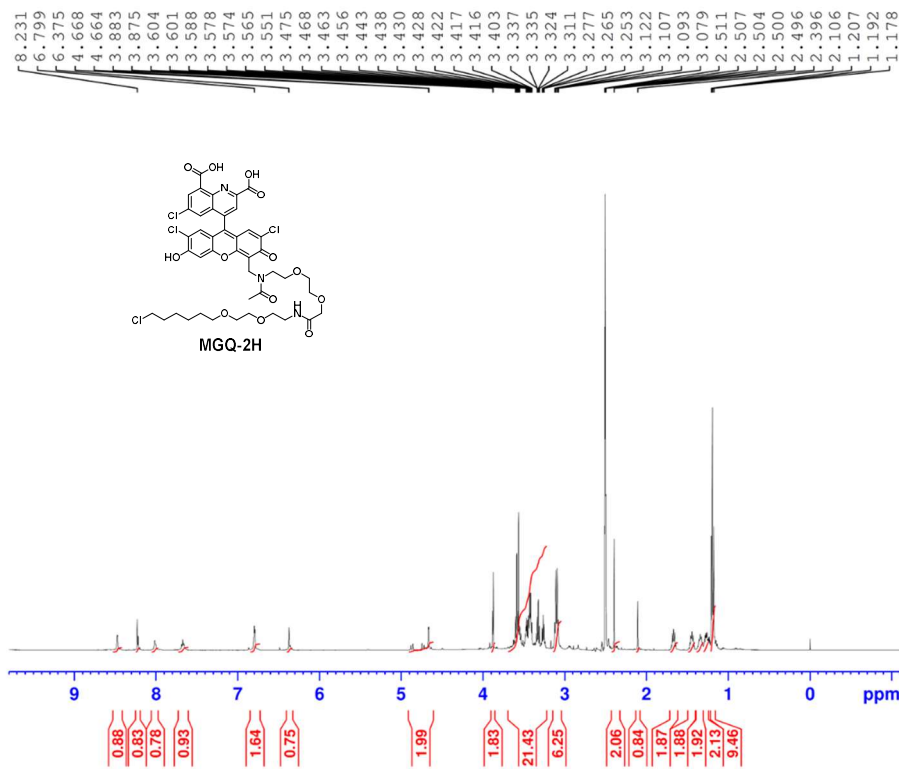
F2 - Acquisition Parameters
 Date_ 20180119
 Time 4.42
 INSTRUM spect
 PROBHD 5 mm CPPBBO BB
 PULPROG zgpg30
 TD 65536
 SOLVENT CDC13
 NS 8192
 DS 4
 SWH 29761.904 Hz
 FIDRES 0.454131 Hz
 AQ 1.1010048 sec
 RG 197.07
 DW 16.800 usec
 DE 18.00 usec
 TE 298.1 K
 D1 2.00000000 sec
 D11 0.03000000 sec
 TD0 1

----- CHANNEL f1 -----
 SFO1 125.7753932 MHz
 NUC1 13C
 P1 10.00 usec
 PLW1 77.00000000 W

----- CHANNEL f2 -----
 SFO2 500.1520006 MHz
 NUC2 1H
 CPDPRG[2] waltz16
 FCPD2 80.00 usec
 PLW2 12.30000019 W
 PLM12 0.43241999 W
 PLM13 0.27675000 W

F2 - Processing parameters
 SI 32768
 SF 125.7628187 MHz
 WDW EM
 SSB 0
 LB 1.00 Hz
 GB 0
 PC 1.40

¹³C NMR spectrum of compound 2



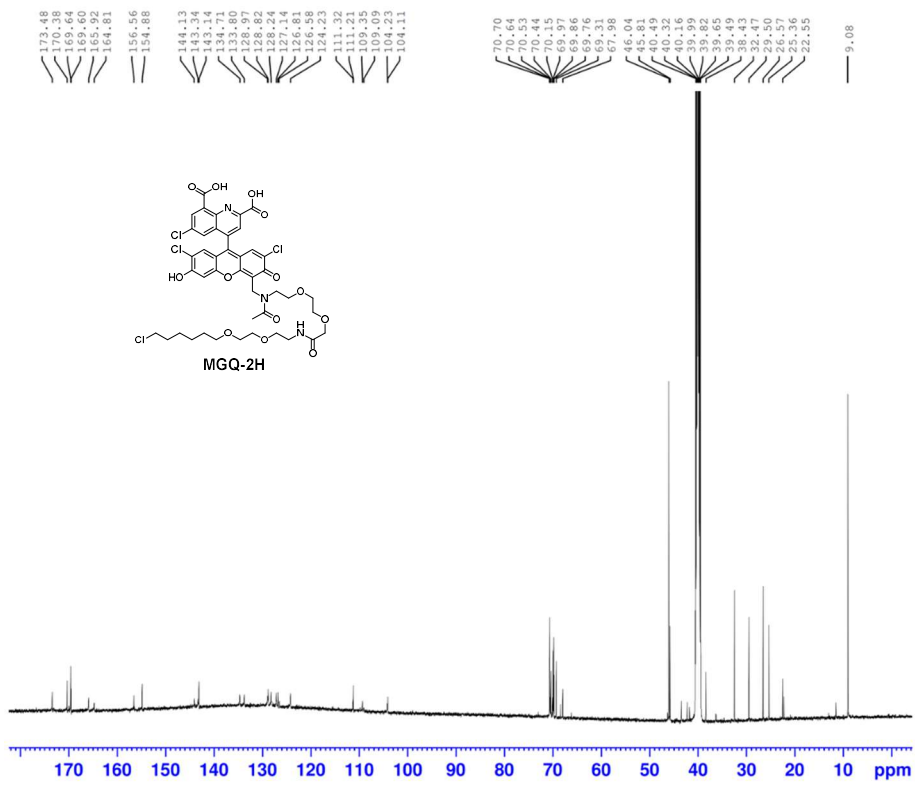
Current Data Parameters
 NAME 20180202MGQ-2-Haalo DMSO
 EXPNO 1
 PROCNO 1

F2 - Acquisition Parameters
 Date_ 20180202
 Time 21.45
 INSTRUM spect
 PROBHD 5 mm CPPBBO BB
 PULPROG zg30
 TD 65536
 SOLVENT DMSO
 NS 2
 DS 16
 SMH 10000.000 Hz
 FIDRES 0.152588 Hz
 AQ 3.274799 sec
 RG 32.16
 DW 50.000 usec
 DE 10.00 usec
 TE 298.2 K
 D1 1.0000000 sec
 TDD 1

===== CHANNEL f1 =====
 SF01 500.153088 MHz
 NUC1 1H
 P1 15.00 usec
 PLW1 12.30000019 W

F2 - Processing parameters
 SI 65536
 SF 500.1500010 MHz
 WDW EM
 SSB 0
 LB 0.30 Hz
 GB 0
 PC 1.00

¹H NMR spectrum of MGQ-2H·Et₃N



Current Data Parameters
 NAME 20180202MGQ-2-Haalo DMSO 13C
 EXPNO 10
 PROCNO 1

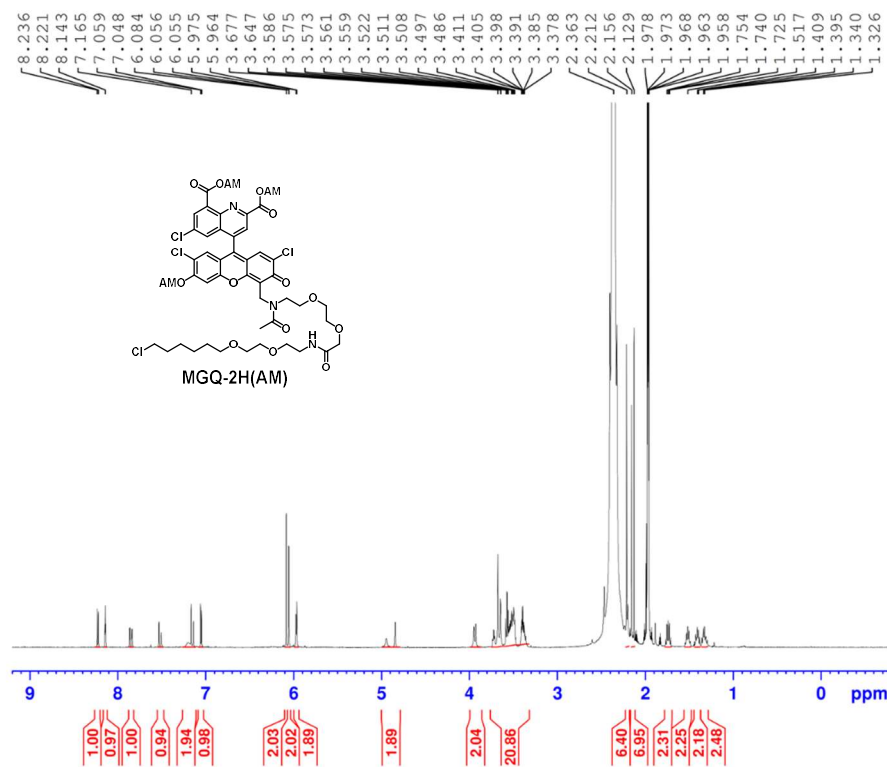
F2 - Acquisition Parameters
 Date_ 20180203
 Time 5.11
 INSTRUM spect
 PROBHD 5 mm CPPBBO BB
 PULPROG zgpg30
 TD 65536
 SOLVENT DMSO
 NS 8192
 DS 4
 SMH 29761.904 Hz
 FIDRES 0.454131 Hz
 AQ 1.1010048 sec
 RG 197.07
 DW 16.800 usec
 DE 18.00 usec
 TE 298.1 K
 D1 2.0000000 sec
 D11 0.63000000 sec
 TDD 1

===== CHANNEL f1 =====
 SF01 125.7753932 MHz
 NUC1 13C
 P1 10.00 usec
 PLW1 77.60000000 W

===== CHANNEL f2 =====
 SF02 500.1520006 MHz
 NUC2 1H
 CPDPRG2 waltz16
 PCPD2 80.00 usec
 PLW2 12.30000019 W
 PLW12 0.43241999 W
 PLW13 0.27675000 W

F2 - Processing parameters
 SI 32768
 SF 125.7628175 MHz
 NDN
 SSB 0
 LB 1.00 Hz
 GB 0
 PC 1.40

¹³C NMR spectrum of MGQ-2H·Et₃N



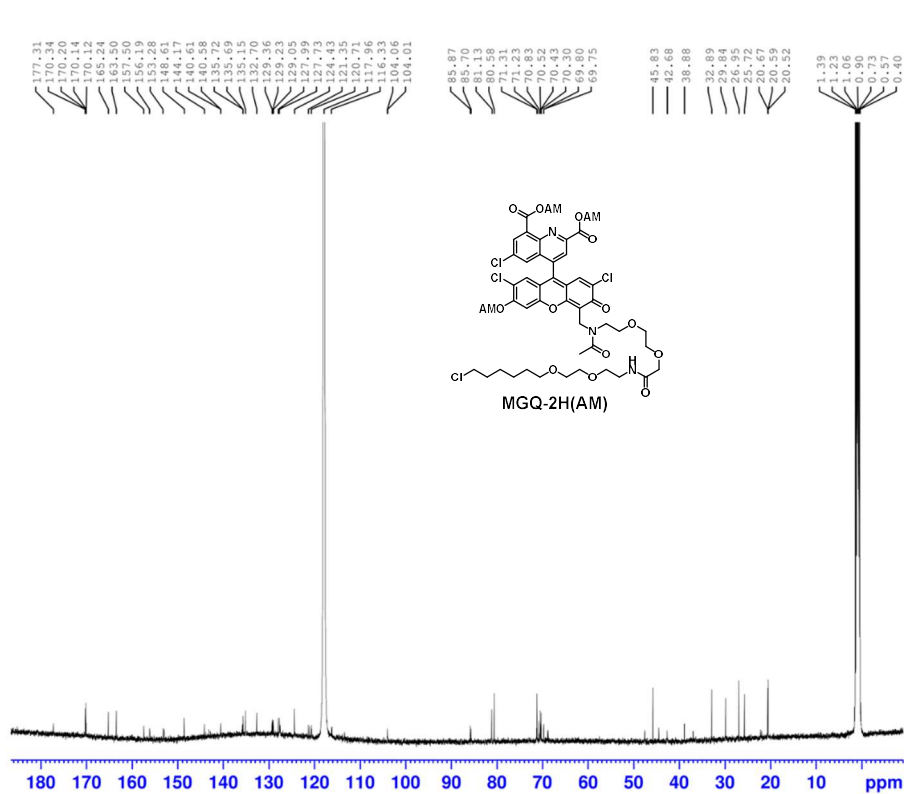
Current Data Parameters
 NAME 20170106compound126 3
 EXPNO 10
 PROCNO 1

F2 - Acquisition Parameters
 Date_ 20170106
 Time 16.08
 INSTRUM spect
 PROBHD 5 mm CFPBBO BB
 PULPROG zg30
 TD 65536
 SOLVENT CD3CN
 NS 16
 DS 2
 SWH 10000.000 Hz
 FIDRES 0.152588 Hz
 AQ 3.2767999 sec
 RG 32.16
 DW 50.000 usec
 DE 10.00 usec
 TE 298.1 K
 D1 1.00000000 sec
 TDO 1

----- CHANNEL f1 -----
 SFO1 500.153086 MHz
 NUC1 1H
 P1 15.00 usec
 PLW1 12.30000019 W

F2 - Processing parameters
 SI 65536
 SF 500.1500000 MHz
 WDW EM
 SSB 0
 LB 0.30 Hz
 GB 0
 PC 1.00

1H NMR spectrum of MGQ-2H(AM)



Current Data Parameters
 NAME 20170106compound126 13C
 EXPNO 20
 PROCNO 1

F2 - Acquisition Parameters
 Date_ 20170107
 Time 10.51
 INSTRUM spect
 PROBHD 5 mm CFPBBO BB
 PULPROG zgpg30
 TD 65536
 SOLVENT CD3CN
 NS 12288
 DS 4
 SWH 29761.904 Hz
 FIDRES 0.454131 Hz
 AQ 1.1010048 sec
 RG 197.07
 DW 16.800 usec
 DE 18.00 usec
 TE 298.2 K
 D1 2.00000000 sec
 D11 0.03000000 sec
 TDO 1

----- CHANNEL f1 -----
 SFO1 125.7753932 MHz
 NUC1 13C
 P1 10.00 usec
 PLW1 77.00000000 W

----- CHANNEL f2 -----
 SFO2 500.1520006 MHz
 NUC2 1H
 CPDPRG2 waltz16
 PCPD2 80.00 usec
 PLW2 12.30000019 W
 PLW12 0.43241999 W
 PLW13 0.27675000 W

F2 - Processing parameters
 SI 32768
 SF 125.7627453 MHz
 WDW EM
 SSB 0
 LB 1.00 Hz
 GB 0
 PC 1.40

13C NMR spectrum of MGQ-2H(AM)